Pain 137 (2008) 495–506

PAIN

www.elsevier.com/locate/pain

Axonal accumulation of hyperpolarization-activated cyclic nucleotide-gated cation channels contributes to mechanical allodynia after peripheral nerve injury in rat

Yu-Qiu Jiang [a,b], Guo-Gang Xing [a], Sheng-Lan Wang [d], Hui-Yin Tu [a], Ye-Nan Chi [a,b], Jie Li [a], Feng-Yu Liu [a,b], Ji-Sheng Han [a,b,c], You Wan [a,b,c,*]

[a] *Neuroscience Research Institute, Peking University, Beijing 100083, China*
[b] *Department of Neurobiology, Peking University, Beijing 100083, China*
[c] *Key Laboratory for Neuroscience, Peking University, Beijing 100083, China*
[d] *Department of Pathology, Peking University, Beijing 100083, China*

Received 8 May 2007; received in revised form 2 September 2007; accepted 8 October 2007

Abstract

Peripheral nerve injury causes neuropathic pain including mechanical allodynia and thermal hyperalgesia due to central and peripheral sensitization. Spontaneous ectopic discharges derived from dorsal root ganglion (DRG) neurons and from the sites of injury are a key factor in the initiation of this sensitization. Numerous studies have focused primarily on DRG neurons; however, the injured axons themselves likely play an equally important role. Previous studies of neuropathic pain rats with spinal nerve ligation (SNL) showed that the hyperpolarization-activated cyclic nucleotide-gated cation (HCN) channel in DRG neuronal bodies is important for the development of neuropathic pain. Here, we investigate the role of the axonal HCN channel in neuropathic pain rats. Using the chronic constriction injury (CCI) model, we found abundant axonal accumulation of HCN channel protein at the injured sites accompanied by a slight decrease in DRG neuronal bodies. The function of these accumulated channels was verified by local application of ZD7288, a specific HCN blocker, which significantly suppressed the ectopic discharges from injured nerve fibers with no effect on impulse conduction. Moreover, mechanical allodynia, but not thermal hyperalgesia, was relieved significantly by ZD7288. These results suggest that axonal HCN channel accumulation plays an important role in ectopic discharges from injured spinal nerves and contributes to the development of mechanical allodynia in neuropathic pain rats.

Keywords: Hyperpolarization-activated cyclic nucleotide-gated cation channel; I_h; Chronic constriction injury (CCI); Neuropathic pain; Ectopic discharge

1. Introduction

Neuropathic pain induced by peripheral nerve injury is characterized by mechanical allodynia, thermal hyperalgesia and spontaneous pain. The mechanisms underlying the development of neuropathic pain behaviors include both peripheral and central sensitization [8,15,41], for which ectopic discharges generated from the injured dorsal root ganglion (DRG) neuronal soma and peripheral axons have been considered to be a major factor [29,44,53].

The mechanisms involved in the generation of ectopic discharges have been studied intensively. A wide range of ion channels have proved to be involved. For example, it was reported that up-regulation of TTX-sensitive

* Corresponding author. Address: Neuroscience Research Institute, Peking University, 38 Xue-Yuan Road, Beijing 100083, China. Tel.: +86 10 8280 5185; fax: +86 10 8280 5185.
E-mail address: ywan@bjmu.edu.cn (Y. Wan).

0304-3959/$34.00
doi:10.1016/j.pain.2007.10.011

$Na_v1.3$ [50,51] was the most critical driving force. In addition, down-regulation of potassium channels was found to be a contributor as well [14,26].

Recently, another interesting ion channel, called hyperpolarization-activated cyclic nucleotide-gated cation channel or HCN channel (referred to as I_h in neurons or I_f in cardiac pacemaker cells), has attracted much attention. First identified in the cardiac sinoatrial node and subsequently in the nervous system, I_h has been found to be involved in a number of neuronal functions, including setting resting membrane potential, participating in pacemaker activity, and modulating synaptic activity [36,39]. Its role in neuropathic pain has also been evaluated. Mayer and Westbrook [32] first identified I_h in DRG neurons, then both our laboratory [49] and others [10] revealed the expression of HCN channels in DRG neurons. In particular, in models of spinal nerve ligation (SNL) and chronic compression of dorsal root ganglion (CCD) [10,55] but not in a sciatic axotomy model [1], I_h was significantly up-regulated in large DRG neurons, accompanied by a paradoxical down-regulation of HCN proteins. Additionally, I_h was found to be involved in the generation of ectopic discharges in DRG neurons [10,45].

The chronic constriction injury (CCI) model is a neuropathic pain model which closely mimics the characteristics of human neuropathic pain behaviors, including mechanical and cold allodynia and heat hyperalgesia [6]. In CCI, ectopic discharges have been detected in both the injured axons at as early as 2 days after injury and later in the DRG neurons [25,37,43,46,54]. Given the relatively superficial location of the injured sciatic nerve, and the critical role of the ectopic discharges generated from this site in the development of neuropathic pain, this model was therefore chosen for our study. Through use of immunohistochemistry, Western blotting, electron microscopy, electrophysiological approaches and behavioral tests, we have demonstrated the abundant axonal accumulation of HCN channels and their contribution to mechanical allodynia, which appears from our work to function through driving spontaneous ectopic discharges.

2. Materials and methods

2.1. Animals

Male Sprague–Dawley rats weighing 250–300 g were used. They were provided by the Department of Experimental Animal Sciences, Peking University Health Science Center. Animals had free access to food and water during experiments and were maintained on natural diurnal cycles. All experiment protocols were approved by the Animal Use and Care Committee of Peking University Health Science Center, which follow the Guidelines of Animal Use and Protection adopted at our university from the National Institutes of Health, USA. Every measure was taken to minimize discomfort to the animals.

2.2. Surgery

In this chronic constrictive injury (CCI) model, loose ligation of the sciatic nerve was performed as previously described [6]. After anesthesia, the left sciatic nerve was exposed at mid-thigh level by blunt dissection through the biceps femoral muscle. Four loosely constrictive (4–0) chromic gut sutures (kindly provided by Prof. Yikuan Xie) were tied around the nerve with spacing at intervals of about 1 mm, then muscles and skin were closed in layers. The contralateral side of each rat was used as control.

2.3. Behavior test

The mechanical and thermal sensitivity of the left hind paw was tested before and after nerve ligation at different time points. The 50% paw withdrawal threshold (PWT) in response to a series of von Frey filaments was examined by the up-down method as described previously [9]. Eight filaments with approximately equal logarithmic incremental (0.224) bending forces were chosen (0.41, 0.70, 1.20, 2.00, 3.63, 5.50, 8.50, and 15.10 g). For thermal hyperalgesia, a method modified from [23] was used for assessing paw-withdrawal latency (PWL) to a thermal stimulus with a mobile radiant heat source. Only those rats with 50% PWT less than 4 g or with a PWL difference between ipsilateral and contralateral hind paws larger than 2 s were selected and used in the subsequent morphological, pharmacological and electrophysiological studies.

2.4. Drug administration

4-(*N*-Ethyl-*N*-phenylamino)-1,2-dimethyl-6-(methylamino) pyrimidinium chloride (ZD7288, molecular weight 292.81, Tocris Cookson, UK) was dissolved and diluted in sterile normal saline to reach the desired concentration (ranging from 5 to 150 $\mu mol \cdot L^{-1}$). For the extracellular electrophysiological recordings, 200 μl of ZD7288 was administered topically to the injured site of the nerve. In the behavioral study, the same volume of the drug was injected perineurally as previously described [47]. Under ether anesthesia, the rat was held in lateral recumbency with the limb to be injected forming a right angle with the longitudinal axis of the trunk. The greater trochanter and ischial tuberosity were localized by palpation. On an imaginary line from the greater trochanter to the ischial tuberosity, at about one third of the distance caudal to the greater trochanter, a 30-gauge injection needle was advanced from the dorsolateral direction at a 45° angle until the tip encountered the ischium. The reagent was maintained at 37 °C before administration. Sterile normal saline was used as control.

2.5. Electron immunomicroscopy

Fourteen days after the CCI operation, two rats with significant mechanical allodynia and heat hyperalgesia were selected for EM study. Short segments of sciatic nerves from about 3 mm central to the most proximal ligation to the second ligation were desheathed and separated longitudinally with No. 5 jewel-

ers forceps, then post-fixed with 4% paraformaldehyde (PFA) for 4 h. After being washed with 0.01 mol · L^{-1} PBS (3 × 5 min), the nerve fibers were blocked with 10% normal goat serum overnight, and then incubated overnight with HCN1 or HCN2 primary antibodies (1:500, 4 °C). For a negative control, the tissues were incubated in 0.01 mol · L^{-1} PBS. The following day, the tissue was rinsed in 0.01 mol · L^{-1} PBS (5 × 10 min), then incubated in Envision buffer (DAKO) for 2 h (20 °C) followed by diaminobenzidine (DAB). The tissue was then post-fixed first in 3% glutaraldehyde (1 h, 4 °C), then in 1% OsO_4 (1 h, 4 °C), and then dehydrated in ascending graded alcohols (4 °C), and embedded in LX-araldite. Longitudinal 70 nm sections were picked up on nickel grids and images were captured with a JEM-1230 electron microscope (JEOL company).

2.6. Immunohistochemistry staining

As described in our previous work [49], the rats were perfused with normal saline followed by 4% paraformaldehyde (PFA) in 0.1 mol · L^{-1} PBS. Bilateral L4 and L5 DRG and sciatic nerves were removed, post-fixed in 4% PFA for 6 h and then dehydrated in 30% sugar solution. Several days later, these tissues were cut in 8-μm-thick serial longitudinal sections and mounted on gelatin/chrome alum-coated glass slides. After blocking in normal goat serum, these sections were incubated overnight at 4 °C with HCN1 or HCN2 primary antibody (1: 1000) (Chemicon), followed by incubation with goat anti-rabbit IgG, and were finally visualized with DAB. The Metamorph software was used for image capture and quantification of cell area.

To measure cell area, each individual neuron including the nuclear region was graphically highlighted. For each subtype of HCN channel, total and positive neurons from 3 sections of each DRG of 3 rats were counted. The percentages of positive neurons to total neurons were calculated and statistically analyzed.

2.7. Western blot analysis

Sciatic nerves or L4 and L5 DRGs were disrupted in lysis buffer (50 mmol · L^{-1} Tris–HCl, 40 mmol · L^{-1}NaF, 2 mmol · L^{-1} EDTA, 1 mmol · L^{-1} DTT with protease inhibitor, pH 7.6). Lysates were separated on SDS–PAGE gels and transferred to PVDF membranes. After blocking with 5% non-fat dried milk in TBST (20 mmol · L^{-1} Tris–HCl, pH 7.5, 150 mmol · L^{-1} NaCl, 0.05% Tween 20), membranes were incubated with rabbit anti-HCN1 (1:3000) or anti-HCN2 (1:1000) antibodies in 5% non-fat dried milk in TBST overnight at 4 °C. After washing with TBST, membranes were incubated with goat anti-rabbit antibody (HRP labeled) diluted with 5% non-fat dried milk in TBST and detected with ECL reagents (Amersham Biosciences, Arlington Heights, IL). Blots were scanned with Spot Advanced and Adobe Photoshop 5.0 (Adobe, Inc.), and band densities were compared with TotalLAB 1.00 software.

2.8. Extracellular electrophysiology

Rats on which the CCI operation had been performed were anesthetized with nembutal (50 mg/kg, *i.p.*). The sciatic nerve was exposed and freed of adherent tissue. Agar (3%) was used to form two small wells on the sciatic nerve at two sites, one about 4–5 cm proximal to the injury site, and just adjacent to the ischium, which was filled with paraffin and used for the placement of recording electrodes. The other well was at the injury site itself for the placement of the stimulating electrode and for application of normal saline (NS) or 50 μmol · L^{-1} ZD7288.

Single unit recording was performed as described in our previous work [44]. Fine axon bundles (microfilaments) were teased from the sciatic nerve centrally with specially honed No. 5 jewelers forceps (Fine Science Tools, Swiss). The cut end of the microfilament was placed on a platinum recording electrode referenced to a nearby indifferent electrode. Any ongoing activity observed in the microfilament was considered as spontaneous afferent activity if gentle mechanical stimuli to skin and muscles innervated by sciatic nerves failed to alter the discharge patterns. Then the observation was extended and the frequency and patterns of firing were registered. The fiber types were classified by conduction velocity: <2 m · s^{-1} for C fibers and $\geqslant 2$ m · s^{-1} for A fibers. Otherwise, we chose an Aβ fiber with spontaneous activity whose firing rate could be altered by stimuli to its receptive field for use in one control study. Data were captured and analyzed with Micro1401 MK II and Spike 2 software (Cambridge Electronic Design, UK).

2.9. Data analysis

Data are expressed as means ± SEM (Standard error of mean). Percentage inhibition of single fiber discharges was analyzed with two-way ANOVA with Bonferroni post-test. Effects on the paw withdrawal threshold and the paw withdrawal latency were analyzed with one-way ANOVA with Dunnett's multiple comparisons, and Western blot results were analyzed with unpaired *t* tests. $p < 0.05$ was considered statistically significant.

3. Results

Chronic constriction injury (CCI) of the sciatic nerve causes a dramatic alteration in morphology and physiology of the injured sciatic nerve as well as in the DRG neurons, with a maximal effect at approximately 2 weeks after nerve injury [2,3,6,19,22]. Accordingly, 10–14 d after nerve injury was chosen as the critical time point in our study. Additionally, our previous work [49] has shown that among the 4 subtypes of HCN channels, HCN1 and HCN2 are the dominant channels in DRG neurons. Therefore, we focused on HCN1 and HCN2.

3.1. Re-distribution of HCN channels in sciatic nerve fibers after CCI

We first examined the expression patterns of HCN1 and HCN2 channel proteins in the DRG neurons with immunohistochemical staining. In agreement with our previous study [49], HCN1 was expressed mainly on the membrane of large and medium-sized DRG neurons (Fig. 1A). HCN2-immunoreactivity (*-ir*) was detected

throughout the small, medium-sized and large DRG neurons (Fig. 1D). It was of interest that the subcellular location of HCN2 was different from that of HCN1, as HCN2-*ir* appeared on the membrane of a few large DRG neurons but was found mostly in the cytoplasm of the medium-sized and small DRG neurons (Fig. 1D, arrows and arrowheads). The expression of HCN1 and HCN2 in DRG neurons was quantified according to cell area, as shown in Fig. 1C and F. It was found that both in the control and CCI rats, HCN1 was distributed prominently in large neurons, while similar percentages of HCN2 were exhibited in different types of neurons. Given that there are more small and the medium-sized neurons than large ones in DRG, we considered HCN2 to be expressed mainly in small and medium-sized neurons.

Expression of these channels was also examined in the normal sciatic nerve. HCN1 expression was too low to be detected with immunohistochemistry staining (Fig. 2D), while HCN2 was found in a linear pattern (Fig. 3D). The subcellular localization of HCN1 in sciatic nerves by electron immunomicroscopy showed strong positive immunolabeling on the axolemma of myelinated thick axons under the high-electron-density myelin (Fig. 4C arrows). However, no positive signal was detected on the axolemma of non-myelinated thin fibers (<1 μm in diameter) or within these fibers (Fig. 4D). In contrast, patchy HCN2 positive staining was more frequently detected on the axolemma of unmyelinated thin fibers (arrows in Fig. 4F), little or no HCN2-*ir* signals were found along the membrane of myelinated thick fibers (Fig. 4E). The negative controls for both anti-HCN1 and HCN2 antibodies showed no positive staining on the membrane of either myelinated or unmyelinated axons (Fig. 4A and B). However due to high electron density, the myelin showed very dark coloration in both negative controls, and in those samples stained with HCN1 or HCN2 antibodies, indicating there was very little or no positive staining in myelin for HCN1/2 protein.

After chronic constriction injury of the sciatic nerves, immunohistochemical staining illustrated a slight reduction of HCN1 and HCN2 expression in large DRG neurons, but the expression of HCN2 in medium-sized and small DRG neurons did not show obvious alteration (Fig. 1B and E). However, the quantification of positive neurons in Fig. 1C and F shows obvious reduction of the percentage of HCN1 and HCN2 positive neurons occurring in all three types of neurons in CCI rats. Moreover, the density of HCN staining in the positive neurons of CCI rats appeared increased in contrast to that of control rats (Fig. 1A, B, D and E).

The changes at the site of sciatic nerve injury were somewhat complex. On day 1 after nerve injury, we could clearly detect four notches on the sciatic nerve as a result of compression by chromic gut sutures, as shown by the four arrows in Figs. 2A and 3A. The magnified figures show that HCN1 proteins appeared to accumulate on the sciatic nerve fibers proximal and distal to the injured site only one day after operation (Figs. 2B and 3B). However, no obvious expression of HCN1 was detected in the area between the ligated sites, and no difference from the control was shown. As for HCN2, there was also an accumulation in the segment proximal

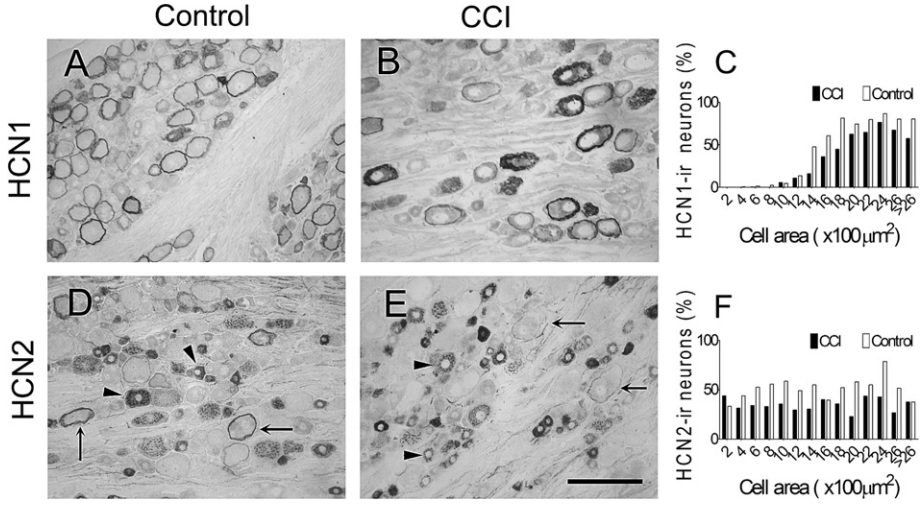

Fig. 1. Immunohistochemical staining of HCN1 and HCN2 in control and injured L4/L5 DRG neurons 14 days after chronic constriction injury (CCI) of the sciatic nerve. (A and D) Show the expression of HCN1 and HCN2 in normal DRGs. HCN1 was expressed predominantly on the membrane of large- and medium-sized DRG neurons (A), while HCN2 was found in neurons of all sizes, and was membrane-positive in large neurons but cytoplasmic in the medium-sized and small neurons (D). (B and E) Show the expression of HCN1 and HCN2 at 14 days after CCI. The percentage of HCN1 positive neurons decreased significantly (B), and statistical results are shown in (C). For HCN2 expression, the HCN2-positive large neurons (arrows) are obviously reduced, while quantification results show broad decreases in small, medium-sized and large neurons (F). Scale bar: 100 μm.

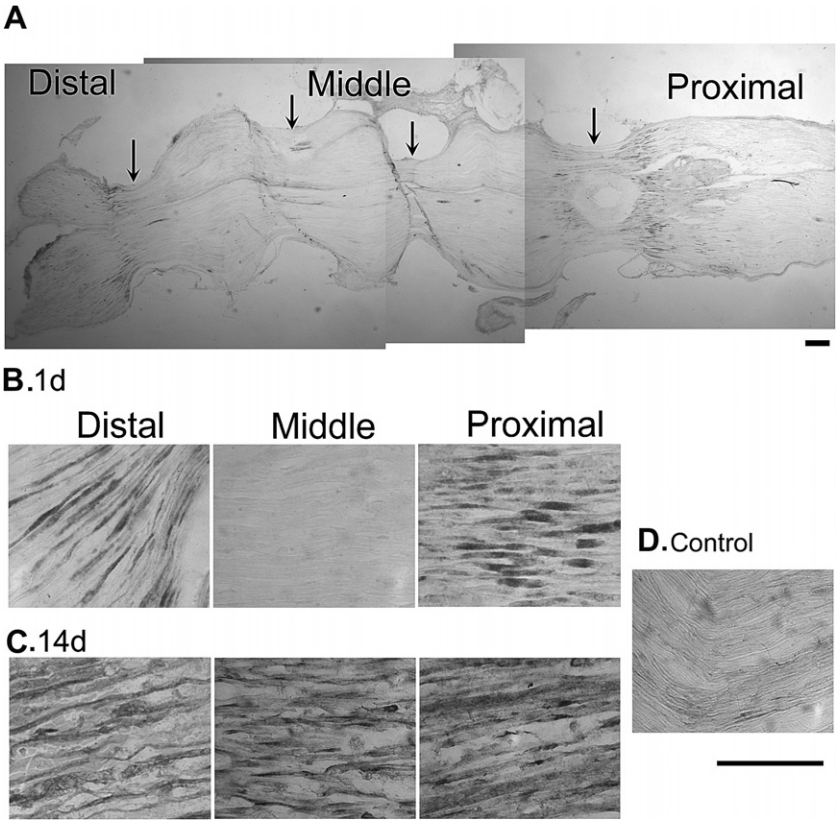

Fig. 2. Immunohistochemical staining of HCN1 in control and chronic constriction injured sciatic nerve fibers. (A) Global view of the injured segment of sciatic nerve fibers extending from the proximal to the distal segment of the injured site 1 day after surgery. Arrows indicate the four compression sites of the ligation. (B) Higher magnification views of the proximal, middle, and distal parts of the injured nerve 1 day after nerve injury. A slight but significant accumulation of HCN1 positive staining can be found in the proximal and distal segments but not in the middle segment. (C) Higher magnification views of the proximal, middle and distal segments of injured nerves at 14 days after surgery. Abundant accumulation of HCN1 positive staining is seen in all three segments of the injured nerve fibers. (D) The expression of HCN1 in normal sciatic nerve fibers as control. Only a small amount of positive staining can be seen. Scale bar: 100 μm.

to the first ligation, but within the ligated and distal segments, the expression of HCN2 seemed similar to that in control nerves. On day 14 after nerve injury, we found that distribution of HCN1 and HCN2 in the proximal, middle and distal parts of the injured nerve fibers appeared to be dense and disordered with a significant reduction of fiber density (Figs. 2C and 3C). For HCN2, we found some clustered positive staining in the proximal and the middle parts of the injured nerve, which may have represented regenerated unmyelinated axons and neuroma-like end-bulbs with HCN2 expression.

In order to quantify the change in HCN channels after CCI, we performed Western blot analysis. First we determined the molecular weight of both HCN1 and HCN2 in the normal brain, DRG and sciatic nerve fibers. Bands with comparable molecular weights of 120 kDa were found in these three different tissues (Fig. 5A and B). In addition, a band of around 100 kDa molecular weight in the brain and DRG could occasionally be detected in low quantity which may be an unglycosylated channel protein as previously reported [33]. The content of both proteins in sciatic nerve fibers was much lower than that in brain and DRG. However, there was a significant increase in both HCN1 and HCN2 proteins in the injured nerves at 14 days after CCI as compared with the uninjured contralateral sciatic nerves, consistent with the findings by immunohistochemical staining. In contrast to the quantification of positive staining of HCN1/2 in DRG neurons, there was no change in either kind of protein in DRG (Fig. 5C and D).

3.2. I_h contributes to the generation of ectopic discharges from the injured sciatic nerve

Next an *in vivo* extracellular single unit recording was performed to determine whether I_h contributes to the ectopic discharges generated from the injured site. Spontaneous discharges from Aβ fibers were recorded from the sciatic nerve on days 10–14 after nerve injury. Similar to that shown in our previous report on the DRG of SNL rats [44], the major patterns of ectopic firing derived from the injured nerves in CCI rats can also be classified into

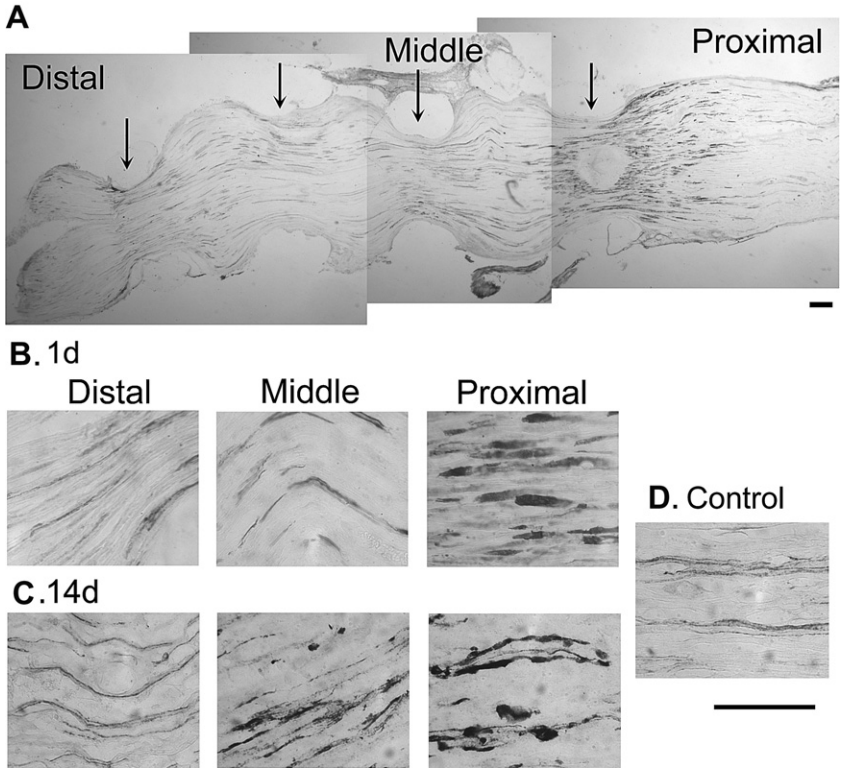

Fig. 3. Immunohistochemical staining of HCN2 expression in control and chronic constriction injured sciatic nerve fibers. Similar to Fig. 2. (A) Global view of the injured segment of sciatic nerve fibers extending from the proximal to the distal segment of the injured site 1 day after surgery. Arrows illustrate the four compression sites induced by ligation. (B) Higher magnification views of the proximal, middle and distal parts of the injured nerve 1 day after CCI. An abundant accumulation of HCN2 positive staining can be found in the proximal, middle and distal parts of the injured sciatic nerve with more predominant expression in the proximal segment. (C) Higher magnification views of the proximal, middle and distal parts of the injured nerves 14 days after surgery. The accumulation is similar to that 1 day after surgery except for some endbulb-like positive dots in the proximal and middle segments. (D) Expression of HCN2 in control sciatic nerves. Slight HCN2 positive staining can be seen which appears to be on the small-diameter fibers. Scale bar: 100 μm.

three types as tonic, burst and irregular. In order to avoid the non-specific effect of ZD7288, we used a relatively low dosage (50 $\mu mol \cdot L^{-1}$), which is enough to inhibit the majority of I_h in dissociated guinea pig substantia nigra neurons [24]. We found that firing frequency was significantly reduced from 16.0 ± 2.1 to 9.4 ± 1.7 Hz (approximately 42% reduction) after topical administration of 50 $\mu mol \cdot L^{-1}$ ZD7288 for 10 min (Fig. 6A and C), and no recovery was observed even 1 h after drug application.

To rule out the possibility that the reduction of ectopic discharges was due to the effect of ZD7288 on conduction in sciatic nerve, a control experiment was performed to test its effect at the same concentration on the conduction of spontaneous activity from the peripheral Aβ-terminals. Thirty minutes after topical application of ZD7288 to the contralateral location corresponding to the ipsilateral injured site, no change in the frequency of spontaneous discharges was observed. However, when ZD7288 was replaced with 2% lidocaine, a non-selective sodium channel blocker, the spontaneous discharges were completely suppressed within 10 min after administration (Fig. 6B). These results strongly support the capacity of ZD7288 for inhibition of the ectopic discharges from the injured Aβ fibers without an effect on impulse conduction. In addition, they help validate the approach to drug administration we used here.

It was of interest that in addition to a direct reduction in firing frequency, we found that ZD7288 could also lead to transformation of discharge patterns. Among the 10 fibers in which ectopic discharges were recorded, most simply manifested decrease of firing frequency. But one sample with tonic discharges, and one with irregular discharges were transformed to bursting discharges after ZD7288 application (Fig. 6E), and another unit with high frequency bursting discharges was transformed to low frequency tonic discharges (Fig. 6D), suggesting that I_h in the injured nerve sites may play a role in the formation of firing patterns.

3.3. ZD7288 relieves mechanical allodynia, but not thermal hyperalgesia

It is widely believed that ectopic discharges generated from the injured site of sciatic nerve in CCI rats

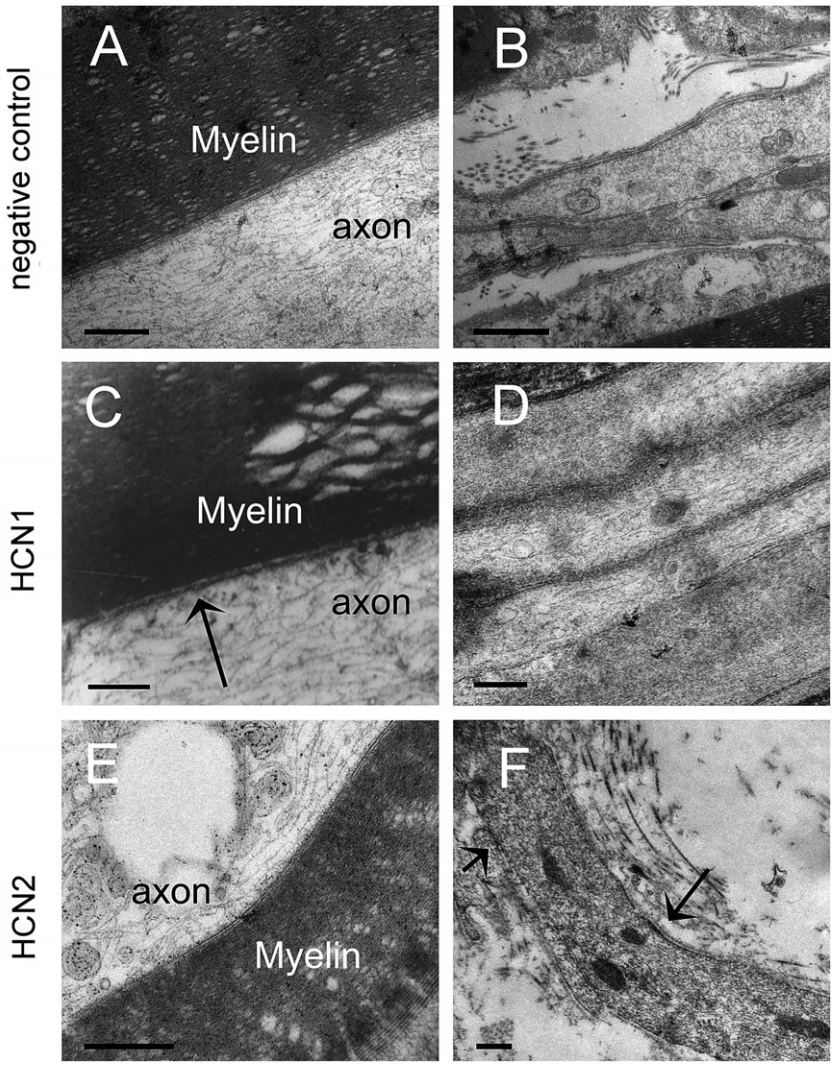

Fig. 4. Electron immunomicroscopy shows the subcellular distribution of HCN1 and HCN2. (A) Negative control of myelinated A fibers without antibodies, note the linear axolemma under the dark myelin with high electron density. (B) Negative control of non-myelinated C fibers without antibodies, also note the linear axolemmas. (C) HCN1-positive staining of the axolemma of myelinated A fibers. Note the segmental positive staining along the membrane under the myelin indicated by arrows. (D) No HCN1-positive staining can be seen on the axolemma of C fibers. (E) No HCN2-positive staining can be seen on the axolemma of A fibers. (F) HCN2-positive staining is found on the axolemma of C fibers with segmental distribution indicated by arrows. Scale bar: 0.5 μm.

play a key role in the development of neuropathic nociceptive behavior [53]. The finding that I_h contributes to the generation of ectopic discharges in injured nerve fibers leads us to question whether I_h in injured sites also plays a role in the development of neuropathic pain behavior. We therefore investigated the effect of I_h antagonist, ZD7288, on pain behavior of CCI rats. Ten to 14 days after operation, rats were used in the behavior study, comparable to those used in the electrophysiological experiment. Four different concentrations of ZD7288 of 5, 15, 50 and 150 $\mu mol \cdot L^{-1}$ were used to test its effect. Behavior testing began at 1 h after perineuronal drug perfusion and the effects were monitored at 2, 4, 8, 12, 24, 48, and 72 h after ZD7288 perfusion. As shown in Fig. 7A and B, it was found that ZD7288 alleviated mechanical allodynia in a dose- and time-dependent manner. The maximal effect was observed at about 8 h after drug perfusion. The analgesic effect was maintained for about 24 h followed by a gradual return to the baseline. To exclude the possibility of a systemic effect of ZD7288, a control experiment was carried out in which the highest dosage of ZD7288 used in these experiments (150 $\mu mol \cdot L^{-1}$) was injected into the contralateral side of CCI rats using the same method of injection. The results showed neither an effect on mechanical allodynia in the ipsilateral hind paw, nor any change in the hypersensitivity in the contralateral hind paw (Fig. 7C), strongly arguing against a systemic effect by ZD7288 in this behavior study. These results also helped confirm that ZD7288 had no effect on the nerve conduction.

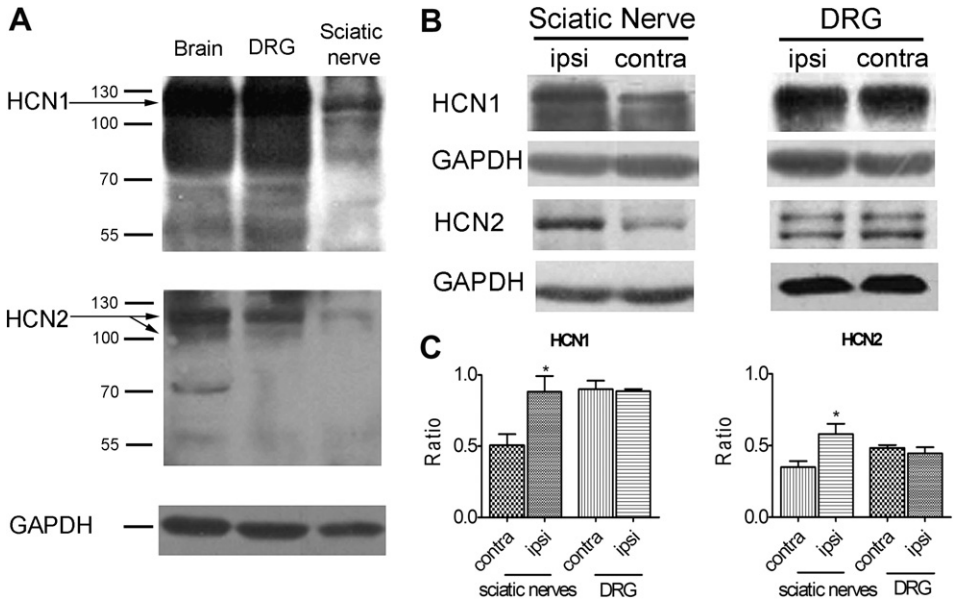

Fig. 5. Western blot analysis of total HCN1 and HCN2 in the injured sciatic nerve fibers and in DRG 14 days after chronic constriction injury. (A) HCN1 and HCN2 in brain, DRG and sciatic nerve fibers. Note each protein shows consistent molecular weight in all three sites, but protein content was significantly higher in the brain and DRG than in sciatic nerves. For HCN2, another band with about 100 kDa molecular weight is present. (B) Immunoreactivity of both HCN1 and HCN2 in the injured (ipsilateral) sciatic nerves increased compared to that in the uninjured nerves (contralateral), and no change in DRG was detected. (C) Statistical analysis of the ratio between HCN1 or HCN2 and GAPDH immunoreactivity. The ratio of HCN1 or HCN2 in the injured sciatic nerves shows increase, but does not change in DRG. $^{*}p < 0.05$, unpaired t-test, $n = 4$.

CCI rats developed a stable thermal hyperalgesia, allowing us to further investigate whether ZD7288 has any effect on thermal hyperalgesia. It was of interest that, even with doses of ZD7288 as high as 150 μmol · L^{-1}, no effect on thermal hyperalgesia was detected (Fig. 8).

4. Discussion

In the present study, by using techniques of immunohistochemistry and Western blot, we have shown for the first time to our knowledge that there are changes in the expression patterns of HCN channel subtypes 1 and 2 in injured peripheral nerves using the CCI model. More importantly, in single unit recording, we found that inhibition of I_h by a specific blocker ZD7288 could profoundly decrease the frequency of ectopic discharges, and behavioral experiments showed that topical application of ZD7288 could significantly relieve mechanical allodynia, but not thermal hyperalgesia. All the above results indicate that the accumulation of HCN channels in primary sensory nerve fibers may play a crucial role in the development of neuropathic pain behavior by driving spontaneous ectopic discharges.

4.1. Change in the expression patterns of HCN channels in primary sensory nerves of CCI rats

Previous histological studies have shown the death of a greater proportion of large neurons than small ones in CCI [3,35]. However, Gabay et al. found an equal reduction in the number of A and C axons conducting past the lesion site 12–15 days after CCI [18], which suggested a similar degree of destruction in A and C fibers, and this observation helps explain the similarly decreased expression of HCN2 in all DRG neurons (Fig. 1). That there was no protein decrease detected in DRG by Western blot analysis (Fig. 4) may be due to some fiber content in the DRG which may express more channel protein after nerve injury. Moreover, it has been reported that I_h was up-regulated in the medium-sized and large TRG neurons 3 days after an infraorbital nerve – CCI operation [27], which suggested increased expression of HCN channels in individual neurons. We also found increased density of HCN channels in positive neurons of the injured DRG as shown in Fig. 1, and this may compensate for the decreased expression in other neurons. The detailed mechanism is unclear and is worthy of further investigation, but inflammatory and neurotrophic factors released by injured neurons and glia are some possible candidate promoters. The most striking finding in this study was the observation of an abundant HCN protein accumulation at the injured site of the sciatic nerve 14 days after nerve injury, leading us to hypothesize a role for this protein in the hyperexcitability of injured sciatic nerves.

4.2. Role of axonal HCN accumulation in the generation of ectopic discharges and neuropathic pain behavior

The ectopic discharges generated from both DRG neurons and the injured nerves in CCI rats are key elements in the development of neuropathic pain [46,53,54]. It has been suggested that endbulbs, sprouts and patches of

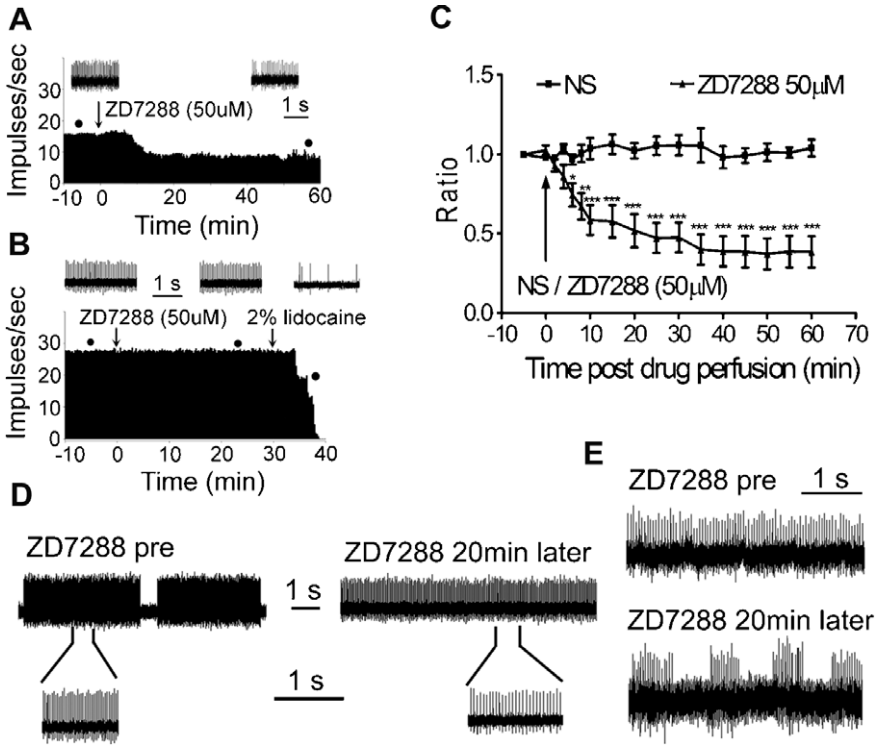

Fig. 6. Inhibition of I_h with ZD7288 suppressed ectopic discharges generated from the injured sciatic nerve fibers. (A) An example of the frequency-time histogram of an ectopic discharge before and after application of ZD7288 at 50 $\mu mol \cdot L^{-1}$ recorded from a single unit of the injured sciatic nerve. Note the significant decrease of discharge frequency 10 min after ZD7288 application. This inhibition lasted for 1 h. (B) An example of the effect of ZD7288 at 50 $\mu mol \cdot L^{-1}$ on spontaneous discharges from the sensory terminals of normal sciatic nerve. No change in the discharge frequency was observed even 30 min after the application of ZD7288, while discharges were strongly suppressed within 10 min of local application of 2% lidocaine. (C) Time course of percentage change of ectopic discharges suppressed by ZD7288 at 50 $\mu mol \cdot L^{-1}$. $^*p < 0.05$, $^{**}p < 0.01$, $^{***}p < 0.001$, two way ANOVA, followed by Bonferroni post-tests, $n = 7$, 10 for NS and ZD7288, respectively. (D and E) Show two examples of the transformation of firing patterns after the application of ZD7288. (d) A burst discharge with high frequency was transformed to low frequency tonic discharge after ZD7288 application. (E) A tonic discharge was transformed to burst discharge.

demyelination distributed in a neuroma became the origination of ectopic discharges [16]. Chronic constriction of sciatic nerve can also undergo such changes. Possible due to the relatively less severe injury in the CCI model, we did not capture endbulbs or sprouts in EM photomicrographs. But the distribution of HCN1 and HCN2 on the axolemma of myelinated and unmyelinated nerve fibers by EM strongly suggested their subcellular location. Several properties of I_h, such as contribution to pacemaker activity, and participation in resting membrane potential, suggest its role in ectopic discharges, and as expected, A-fiber ectopic discharges were partially inhibited by local administration of ZD7288 in our study, consistent with previous experiments carried out on DRG neurons in SNL rats [10,45].

Our behavior tests showed that local application of ZD7288 significantly inhibited mechanical allodynia in a time- and dose-dependent manner, which seems similar to a previous study on the SNL model with systemic administration of ZD7288 [10]. Nevertheless, HCN channels (or I_h) are widely expressed throughout the peripheral and central nervous systems [21,31,39,49]. Moreover, ZD7288 can inhibit synaptic activity via non-specific effect on NMDA and AMPA receptors [11], and our recent work also demonstrated the analgesic effect of ZD7288 by intrathecal injection in SNL rats, raising a question about the systemic effect of ZD7288 [48]. However, in the present study, ZD7288 was directly applied to the sciatic nerve, and no effect was identified in contralateral administration, both of which help exclude the possibility of central or systemic effects. Another concern regarding ZD7288 stems from a recent finding that this drug inhibits T-type calcium channels [17]. However, the dosage used to block T-type calcium channel in that study was much higher than that used here. Taken together, we conclude that peripheral HCN channels (or I_h) are responsible for mechanical allodynia in CCI rats via participation in the generation of ectopic discharges in the injured nerve fibers.

No effect of ZD7288 on thermal hyperalgesia was found in the present study, which is presumably due to the minor role of A-fiber ectopic discharges as compared with sensitized C afferents in thermal hyperalgesia [42], and suggests that axonal accumulated HCN channels in C fibers might not be functional in C afferent sensitization. However, this speculation needs further investigation.

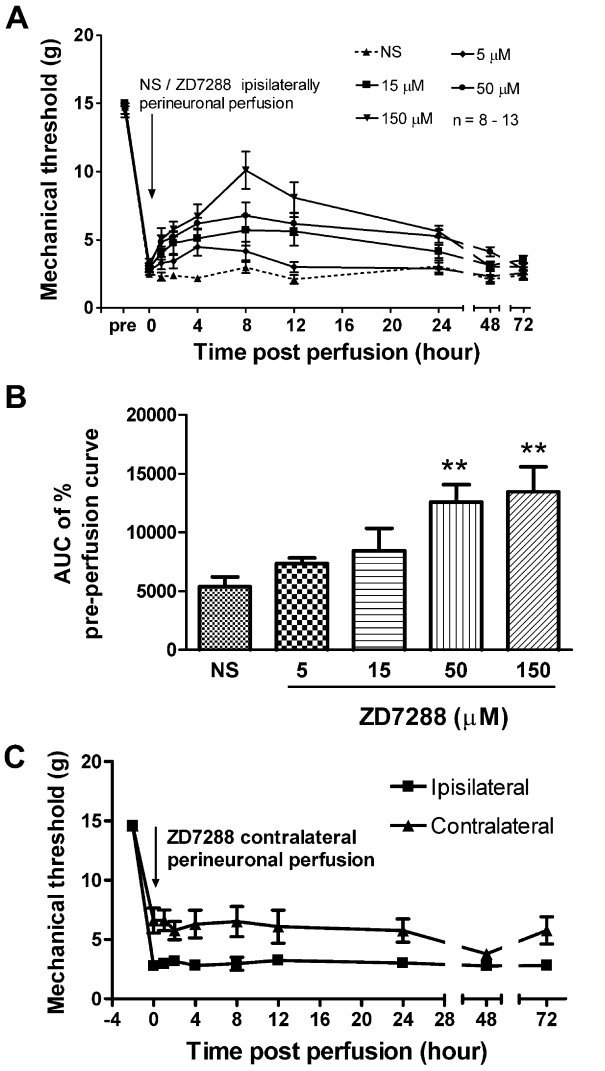

Fig. 7. Effect of perineuronal perfusion of ZD7288 on mechanical allodynia at 14 days after nerve injury. (A) ZD7288 partially reversed the mechanical allodynia in a dose- and time-dependent manner. $n = 8$–13. (B) Statistical analysis using area under the curve of percentage change of maximum possible effect (% MPE). $*p < 0.05$, $**p < 0.01$, $***p < 0.001$, one way ANOVA with Dunnett's multiple comparisons. (C) Effect of contralateral perineuronal perfusion of ZD7288 at 150 $\mu mol \cdot L^{-1}$ on ipsilateral mechanical allodynia. No significant change in the paw withdrawal threshold was observed in either the ipsilateral or contralateral side, excluding a systemic effect of ZD7288 on ipsilateral mechanical allodynia. $n = 8$.

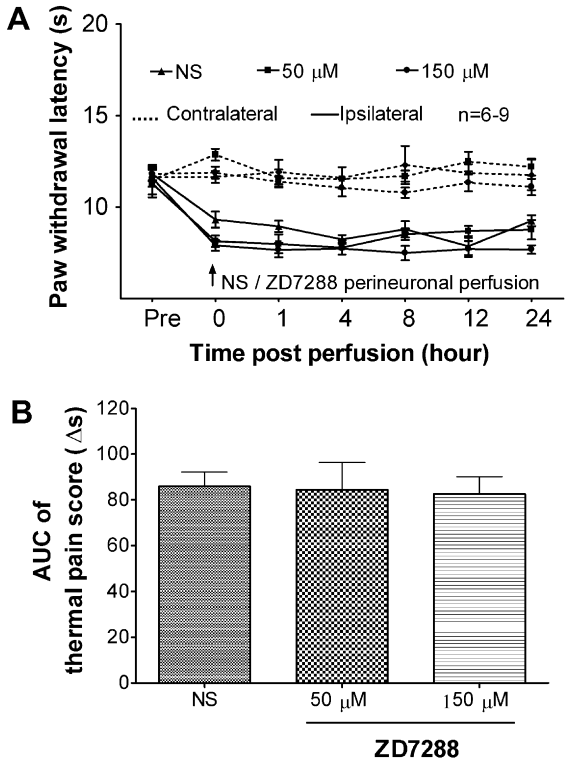

Fig. 8. Effect of perineuronal perfusion of ZD7288 on thermal hyperalgesia 14 days after nerve injury. (A) ZD7288 at 50 and 150 $\mu mol \cdot L^{-1}$ did not show any effect on shortening of paw withdrawal latency (thermal hyperalgesia) compared with normal saline (NS). (B) Statistical analysis with area under the curve (AUC) of the effect of ZD7288 on the ipsilateral paw withdrawal latency. No significant difference was observed between ZD7288 at 50 or 150 $\mu mol \cdot L^{-1}$ and normal saline (NS).

In addition, a previous report identified I_h in cold-response but not heat-response C-fibers [5], so inhibition of I_h by ZD7288 may be effective in inhibition of cold allodynia, which is another prominent characteristics developed in CCI rats.

4.3. A comparison of distribution patterns and roles of HCN channels and sodium channels after peripheral nerve injury

The redistribution of ion channels has been reported in various neuropathic pain models and in human neuropathic pain patients. Most importantly, $Na_v1.8$, the major TTX-resistant sodium channel expressed in small DRG neurons, was found to undergo redistribution from DRG neurons to the injured nerve fibers in CCI models, neuroma model, brachial plexus injury patients and human neuroma [12,28,34,38,40]. In SNL rats, $Na_v1.8$ was reported to redistribute to uninjured sciatic nerves [20] and to L4 DRG neurons [38], or to undergo no redistribution at all [13]. Subsequent studies confirmed that the redistributed $Na_v1.8$ channels were important for the development of neuropathic pain through participation in sensitization of uninjured C or Aδ afferents [20,52].

In this study, HCN1 channels (Fig. 1A and B), as well as I_h, are expressed mainly on the membrane of large and medium-sized DRG neuronal soma [49], and HCN1 can be found to accumulate on the axolemma of myelinated axons only after constrictive injury. As for HCN2, though a small percentage of HCN2-*ir* was present on the membrane of large DRG neurons, most HCN2-*ir* was detected in the cytoplasm of small and some medium-sized neurons (Fig. 1D and E). By con-

trast, we found definite expression, although in lower quantity of HCN2 on the axolemma of normal sciatic nerve fibers, which was more abundant after nerve injury. The differences in distribution patterns of HCN1 and HCN2 in normal and injured DRG neurons and fibers are very interesting, and suggest distinct roles for HCN1 and HCN2 in the peripheral nervous system. I_h mediated by HCN1 channels functions mainly in stabilization of resting membrane potential in normal neuronal soma, and acts as a pacemaker in injured Aβ afferents. However, I_h mediated by HCN2 may function mainly in peripheral axons of DRG neurons, serve as a modulator of C and Aδ fibers conduction in normal conditions, and contribute to the hyperexcitability of the uninjured C fibers after nerve injury. Further evidence may be collected when subtype-specific blockers or transgenic techniques such as RNA interference *in vivo* become available.

4.4. Possible mechanisms of accumulation of HCN channels

The mechanism involved in axonal HCN accumulations remains largely unclear, but may be similar to that proposed in sodium channel accumulation. For instance, partial blockade of antrograde and retrograde axonal transport may play a role. This phenomenon has been found to operate with sodium and potassium channels after ligation of sciatic nerves [4,30]. Second, regenerated axons and new axonal sprouts following sciatic nerve injury are likely to express more HCN channels [19,22]. Third, neurotrophic factors released from activated Schwann cells and macrophagocytes at the injured site [7] may also be modulators of HCN channels' expression and translocation.

In conclusion, our present data strongly suggest that axonal HCN accumulation following CCI plays an important role in the development of neuropathic pain via driving ectopic discharges. This study, together with our previous findings, and the work of others [10,45,49,55], suggests that I_h may be a potential peripheral target for the treatment of neuropathic pain.

Acknowledgements

This project was supported by grants from the National Natural Science Foundation of China (30470559, 30330230) and Beijing Natural Science Foundation (7052039). Authors would like to thank Prof. Michael A. McNutt in the Department of Pathology Peking University Health Science Center, and Dr. Qian Sun in Brandeis University, USA for his help in the preparation of this manuscript.

References

[1] Abdulla FA, Smith PA. Axotomy- and autotomy-induced changes in Ca^{2+} and K^+ channel currents of rat dorsal root ganglion neurons. J Neurophysiol 2001;85:644–58.
[2] Attal N, Filliatreau G, Perrot S, Jazat F, Di Giamberardino L, Guilbaud G. Behavioural pain-related disorders and contribution of the saphenous nerve in crush and chronic constriction injury of the rat sciatic nerve. Pain 1994;59:301–12.
[3] Basbaum AI, Gautron M, Jazat F, Mayes M, Guilbaud G. The spectrum of fiber loss in a model of neuropathic pain in the rat: an electron microscopic study. Pain 1991;47:359–67.
[4] Bearzatto B, Lesage F, Reyes R, Lazdunski M, Laduron PM. Axonal transport of TREK and TRAAK potassium channels in rat sciatic nerves. Neuroreport 2000;11:927–30.
[5] Beggs S, Koltzenburg M, Pracher F. Heat sensitivity of mouse C-fibre afferents as a predictor of use-dependent slowing. In Proceedings of the 10th World Congress on Pain, San Diego, CA, 2002. Abstract.
[6] Bennett GJ, Xie YK. A peripheral mononeuropathy in rat that produces disorders of pain sensation like those seen in man. Pain 1988;33:87–107.
[7] Campana WM. Schwann cells: activated peripheral glia and their role in neuropathic pain. Brain Behav Immun 2007. Epub. ahead of print.
[8] Campbell JN, Meyer RA. Mechanisms of neuropathic pain. Neuron 2006;52:77–92.
[9] Chaplan SR, Bach FW, Pogrel JW, Chung JM, Yaksh TL. Quantitative assessment of tactile allodynia in the rat paw. J. Neurosci Methods 1994;53:55–63.
[10] Chaplan SR, Guo HQ, Lee DH, Luo L, Liu C, Kuei C, et al. Neuronal hyperpolarization-activated pacemaker channels drive neuropathic pain. J Neurosci 2003;23:1169–78.
[11] Chen C, Cavanaugh JM, Song Z, Takebayashi T, Kallakuri S, Wooley PH. Effects of nucleus pulposus on nerve root neural activity, mechanosensitivity, axonal morphology, and sodium channel expression. Spine 2004;29:17–25.
[12] Coward K, Plumpton C, Facer P, Birch R, Carlstedt T, Tate S, et al. Immunolocalization of SNS/PN3 and NaN/SNS2 sodium channels in human pain states. Pain 2000;85:41–50.
[13] Decosterd I, Ji RR, Abdi S, Tate S, Woolf CJ. The pattern of expression of the voltage-gated sodium channels Na(v)1.8 and Na(v)1.9 does not change in uninjured primary sensory neurons in experimental neuropathic pain models. Pain 2002;96:269–77.
[14] Devor M. Potassium channels moderate ectopic excitability of nerve-end neuromas in rats. Neurosci Lett 1983;40:181–6.
[15] Devor M. Neuropathic pain and injured nerve: peripheral mechanisms. Br Med Bull 1991;47:619–30.
[16] Devor M. The pathophysiology and anatomy of damaged nerve. In: Wall PD, Melzack R, editors. Textbook of Pain, 1984. p. 49–64.
[17] Felix R, Sandoval A, Sanchez D, Gomora JC, Vega-Beltran JL, Trevino CL, et al. ZD7288 inhibits low-threshold Ca^{2+} channel activity and regulates sperm function. Biochem Biophys Res Commun 2003;311:187–92.
[18] Gabay E, Tal M. Pain behavior and nerve electrophysiology in the CCI model of neuropathic pain. Pain 2004;110:354–60.
[19] Gautron M, Jazat F, Ratinahirana H, Hauw JJ, Guilbaud G. Alterations in myelinated fibres in the sciatic nerve of rats after constriction: possible relationships between the presence of abnormal small myelinated fibres and pain-related behaviour. Neurosci Lett 1990;111:28–33.
[20] Gold MS, Weinreich D, Kim CS, Wang R, Treanor J, Porreca F, et al. Redistribution of Na(V)1.8 in uninjured axons enables neuropathic pain. J. Neurosci 2003;23:158–66.
[21] Grafe P, Quasthoff S, Grosskreutz J, Alzheimer C. Function of the hyperpolarization-activated inward rectification in nonmyelinated peripheral rat and human axons. J Neurophysiol 1997;77:421–6.

[22] Guilbaud G, Gautron M, Jazat F, Ratinahirana H, Hassig R, Hauw JJ. Time course of degeneration and regeneration of myelinated nerve fibres following chronic loose ligatures of the rat sciatic nerve: can nerve lesions be linked to the abnormal pain-related behaviours? Pain 1993;53:147–58.
[23] Hargreaves K, Dubner R, Brown F, Flores C, Joris J. A new and sensitive method for measuring thermal nociception in cutaneous hyperalgesia. Pain 1988;32:77–88.
[24] Harris NC, Constanti A. Mechanism of block by ZD 7288 of the hyperpolarization-activated inward rectifying current in guinea pig substantia nigra neurons in vitro. J Neurophysiol 1995;74:2366–78.
[25] Kajander KC, Bennett GJ. Onset of a painful peripheral neuropathy in rat: a partial and differential deafferentation and spontaneous discharge in A beta and A delta primary afferent neurons. J Neurophysiol 1992;68:734–44.
[26] Kim DS, Choi JO, Rim HD, Cho HJ. Downregulation of voltage-gated potassium channel alpha gene expression in dorsal root ganglia following chronic constriction injury of the rat sciatic nerve. Brain Res Mol Brain Res 2002;105:146–52.
[27] Kitagawa J, Takeda M, Suzuki I, Kadoi J, Tsuboi Y, Honda K, et al. Mechanisms involved in modulation of trigeminal primary afferent activity in rats with peripheral mononeuropathy. Eur J Neurosci 2006;24:1976–86.
[28] Kretschmer T, Happel LT, England JD, Nguyen DH, Tiel RL, Beuerman RW, et al. Accumulation of PN1 and PN3 sodium channels in painful human neuroma-evidence from immunocytochemistry. Acta Neurochir (Wien) 2002;144:803–10.
[29] Liu CN, Wall PD, Ben Dor E, Michaelis M, Amir R, Devor M. Tactile allodynia in the absence of C-fiber activation: altered firing properties of DRG neurons following spinal nerve injury. Pain 2000;85:503–21.
[30] Lombet A, Laduron P, Mourre C, Jacomet Y, Lazdunski M. Axonal transport of the voltage-dependent Na^+ channel protein identified by its tetrodotoxin binding site in rat sciatic nerves. Brain Res 1985;345:153–8.
[31] Luo L, Chang L, Brown SM, Ao H, Lee DH, Higuera ES, et al. Role of peripheral hyperpolarization-activated cyclic nucleotide-modulated channel pacemaker channels in acute and chronic pain models in the rat. Neuroscience 2007;144:1477–85.
[32] Mayer ML, Westbrook GL. A voltage-clamp analysis of inward (anomalous) rectification in mouse spinal sensory ganglion neurones. J Physiol 1983;340:19–45.
[33] Much B, Wahl-Schott C, Zong X, Schneider A, Baumann L, Moosmang S, et al. Role of subunit heteromerization and N-linked glycosylation in the formation of functional hyperpolarization-activated cyclic nucleotide-gated channels. J Biol Chem 2003;278:43781–6.
[34] Novakovic SD, Tzoumaka E, McGivern JG, Haraguchi M, Sangameswaran L, Gogas KR, et al. Distribution of the tetrodotoxin-resistant sodium channel PN3 in rat sensory neurons in normal and neuropathic conditions. J Neurosci 1998;18:2174–87.
[35] Obata K, Yamanaka H, Fukuoka T, Yi D, Tokunaga A, Hashimoto N, et al. Contribution of injured and uninjured dorsal root ganglion neurons to pain behavior and the changes in gene expression following chronic constriction injury of the sciatic nerve in rats. Pain 2003;101:65–77.
[36] Pape HC. Queer current and pacemaker: the hyperpolarization-activated cation current in neurons. Annu Rev Physiol 1996;58:299–327. 299–327.
[37] Petersen M, Zhang J, Zhang JM, LaMotte RH. Abnormal spontaneous activity and responses to norepinephrine in dissociated dorsal root ganglion cells after chronic nerve constriction. Pain 1996;67:391–7.
[38] Porreca F, Lai J, Bian D, Wegert S, Ossipov MH, Eglen RM, et al. A comparison of the potential role of the tetrodotoxin-insensitive sodium channels, PN3/SNS and NaN/SNS2, in rat models of chronic pain. Proc Natl Acad Sci USA 1999;96:7640–4.
[39] Robinson RB, Siegelbaum SA. Hyperpolarization-activated cation currents: from molecules to physiological function. Annu Rev Physiol 2003;65:453–80.
[40] Roza C, Laird JM, Souslova V, Wood JN, Cervero F. The tetrodotoxin-resistant Na^+ channel $Na_v1.8$ is essential for the expression of spontaneous activity in damaged sensory axons of mice. J Physiol 2003;550:921–6.
[41] Scholz J, Woolf CJ. Can we conquer pain? Nat Neurosci 2002;5(Suppl):1062–7.
[42] Shir Y, Seltzer Z. A-fibers mediate mechanical hyperesthesia and allodynia and C-fibers mediate thermal hyperalgesia in a new model of causalgiform pain disorders in rats. Neurosci Lett 1990;115:62–7.
[43] Study RE, Kral MG. Spontaneous action potential activity in isolated dorsal root ganglion neurons from rats with a painful neuropathy. Pain 1996;65:235–42.
[44] Sun Q, Tu H, Xing GG, Han JS, Wan Y. Ectopic discharges from injured nerve fibers are highly correlated with tactile allodynia only in early, but not late, stage in rats with spinal nerve ligation. Exp Neurol 2005;191:128–36.
[45] Sun Q, Xing GG, Tu HY, Han JS, Wan Y. Inhibition of hyperpolarization-activated current by ZD7288 suppresses ectopic discharges of injured dorsal root ganglion neurons in a rat model of neuropathic pain. Brain Res 2005;1032:63–9.
[46] Tal M, Eliav E. Abnormal discharge originates at the site of nerve injury in experimental constriction neuropathy (CCI) in the rat. Pain 1996;64:511–8.
[47] Thalhammer JG, Vladimirova M, Bershadsky B, Strichartz GR. Neurologic evaluation of the rat during sciatic nerve block with lidocaine. Anesthesiology 1995;82:1013–25.
[48] Tu H, Jiang YQ, Liu FY, Xing GG, Shi YS, Li T, et al. The effects of intrathecal application of ZD7288, and HCN blocker, on mechanical allodynia of neuropathic pain model rats. Chin J Pain Med 2006;12:228–33.
[49] Tu H, Deng L, Sun Q, Yao L, Han JS, Wan Y. Hyperpolarization-activated, cyclic nucleotide-gated cation channels: roles in the differential electrophysiological properties of rat primary afferent neurons. J Neurosci Res 2004;76:713–22.
[50] Waxman SG, Dib-Hajj S, Cummins TR, Black JA. Sodium channels and pain. Proc Natl Acad Sci USA 1999;96:7635–9.
[51] Waxman SG, Kocsis JD, Black JA. Type III sodium channel mRNA is expressed in embryonic but not adult spinal sensory neurons, and is reexpressed following axotomy. J Neurophysiol 1994;72:466–70.
[52] Wu G, Ringkamp M, Hartke TV, Murinson BB, Campbell JN, Griffin JW, et al. Early onset of spontaneous activity in uninjured C-fiber nociceptors after injury to neighboring nerve fibers. J Neurosci 2001;21:RC140.
[53] Xie W, Strong JA, Meij JT, Zhang JM, Yu L. Neuropathic pain: early spontaneous afferent activity is the trigger. Pain 2005;116:243–56.
[54] Xie Y, Zhang J, Petersen M, LaMotte RH. Functional changes in dorsal root ganglion cells after chronic nerve constriction in the rat. J Neurophysiol 1995;73:1811–20.
[55] Yao H, Donnelly DF, Ma C, LaMotte RH. Upregulation of the hyperpolarization-activated cation current after chronic compression of the dorsal root ganglion. J Neurosci 2003;23:2069–74.